ChemEurJ

Research Article
doi.org/10.1002/chem.202502670

Chemistry Europe
European Chemical Societies Publishing

www.chemeurj.org

Binding of Tetrapentylammonium to a c-MYC G-quadruplex Depicted through NMR and Volumetric Assessment

Xuan Li,[a] Mirko Cevec,[b] David N. Dubins,[a] Janez Plavec,*[b] and Tigran V. Chalikian*[a]

We recently have demonstrated that, their structural simplicity notwithstanding, tetraalkylammonium (TAA^+) ions, *i.e.*, $[H(CH_2)_n]_4N^+$, strongly stabilize the parallel c-MYC G-quadruplex while not affecting the thermal stabilities of the antiparallel human telomeric G-quadruplex or duplex DNA. In the present work, we expand on our discovered paradigm of topology-selective G-quadruplex recognition by performing NMR spectroscopic and volumetric characterization of the complex between tetrapentylammonium ($TPeA^+$) and the c-MYC G-quadruplex. The binding of TAA^+ to the c-MYC G-quadruplex is optically silent, which necessitates the use of nonoptical observables, such as density and sound velocity. Our NMR results revealed that $TPeA^+$ forms a stable complex with the c-MYC G-quadruplex in which the ligand is positioned above the G9-G13-G18-G22 quartet and is surrounded by the 3′-(T23-A24-A25) flanking region. We used our densimetric and ultrasonic velocimetric results to calculate changes in volume, ΔV, and adiabatic compressibility, ΔK_S, accompanying the binding of $TPeA^+$ to the c-MYC G-quadruplex. We rationalized these volumetric properties to determine binding-induced changes in hydration of the associating molecules and the internal dynamics of the host G-quadruplex. In general, the structural and physico-chemical insights emerging from this work lay the foundation for further studies of TAA^+-based compounds as a possible starting point for designing topology-sensitive G-quadruplex-binding agents.

1. Introduction

G-quadruplexes are tetrahelical, noncanonical secondary structures that are formed by single-stranded stretches of DNA rich in guanine.[1–5] The building block of a G-quadruplex is a G-quartet, a planar structure in which four guanine bases interlink in a circular manner *via* Hoogsteen hydrogen bonds.[2,4,6] A typical G-quadruplex involves two or more G-quartets which stack upon each other, thereby producing a central cavity lined with four guanine O6 oxygen atoms.[2] G-quadruplexes are stabilized additionally by cations of the appropriate radius, usually Na^+ or K^+, which are coordinated to the O6 atoms in the central cavity.[2,6–11]

There are hundreds of thousands of G-quadruplex-forming sequences in the genome, and these sequences are overrepresented in regions of critical importance and biological control such as the promoter regions of many oncogenes.[1,12–14] Growing evidence suggests that G-quadruplexes participate in the regulation of genomic events such as gene transcription and translation, DNA replication, telomere homeostasis, *etc.*[3,13–16] In this respect, we have proposed that G-quadruplex-based regulation of genomic events is under thermodynamic control.[17–20] Given the regulatory role of G-quadruplexes, drug-induced stabilization of these noncanonical structures has been considered as one plausible way to control their participation in genomic events.[1,21–24] To this end, a large number of G-quadruplex-selective ligands have been designed and investigated *in vitro* and *in vivo*.[1,22,25–27] Such ligands are, generally, positively charged aromatic compounds targeting G-quartet as their main recognition element.[21,27–29]

G-quadruplexes differ in topology, which is determined by the relative orientation of G-tracks (parallel, antiparallel, hybrid); a recurrent challenge of development of G-quadruplex-selective drugs is to endow them with the ability to discriminate between different topologies.[2,30,31] Tetraalkylammonium (TAA^+) salts, which are used widely as buffer components, have never been assumed to have direct interactions with G-quadruplexes. Contrary to this generally accepted view, however, we have demonstrated that, despite their simplicity, TAA^+ salts do interact directly with G-quadruplexes in a topology-selective manner.[32] Specifically, we have explored the effect of a series of TAA^+ ions, *i.e.*, $[H(CH_2)_n]_4N^+$, on the thermal stabilities of the parallel c-MYC G-quadruplex (formed by the modified c-MYC sequence MYC22-G14T/G23T with two G-to-T mutations), the basket-type antiparallel human telomeric G-quadruplex, and duplex DNA.[32] We found that TAA^+ ions strongly stabilize the c-MYC G-quadruplex while not affecting the stabilities of

[a] X. Li, D. N. Dubins, T. V. Chalikian
Department of Pharmaceutical Sciences, Leslie Dan Faculty of Pharmacy, University of Toronto, 144 College Street, Toronto, Ontario M5S 3M2, Canada
E-mail: t.chalikian@utoronto.ca

[b] M. Cevec, J. Plavec
Slovenian NMR Centre, National Institute of Chemistry, Hajdrihova 19, Ljubljana 1000, Slovenia
E-mail: janez.plavec@ki.si

Xuan Li and Mirko Cevec contributed equally to this work.

Supporting information for this article is available on the WWW under https://doi.org/10.1002/chem.202502670

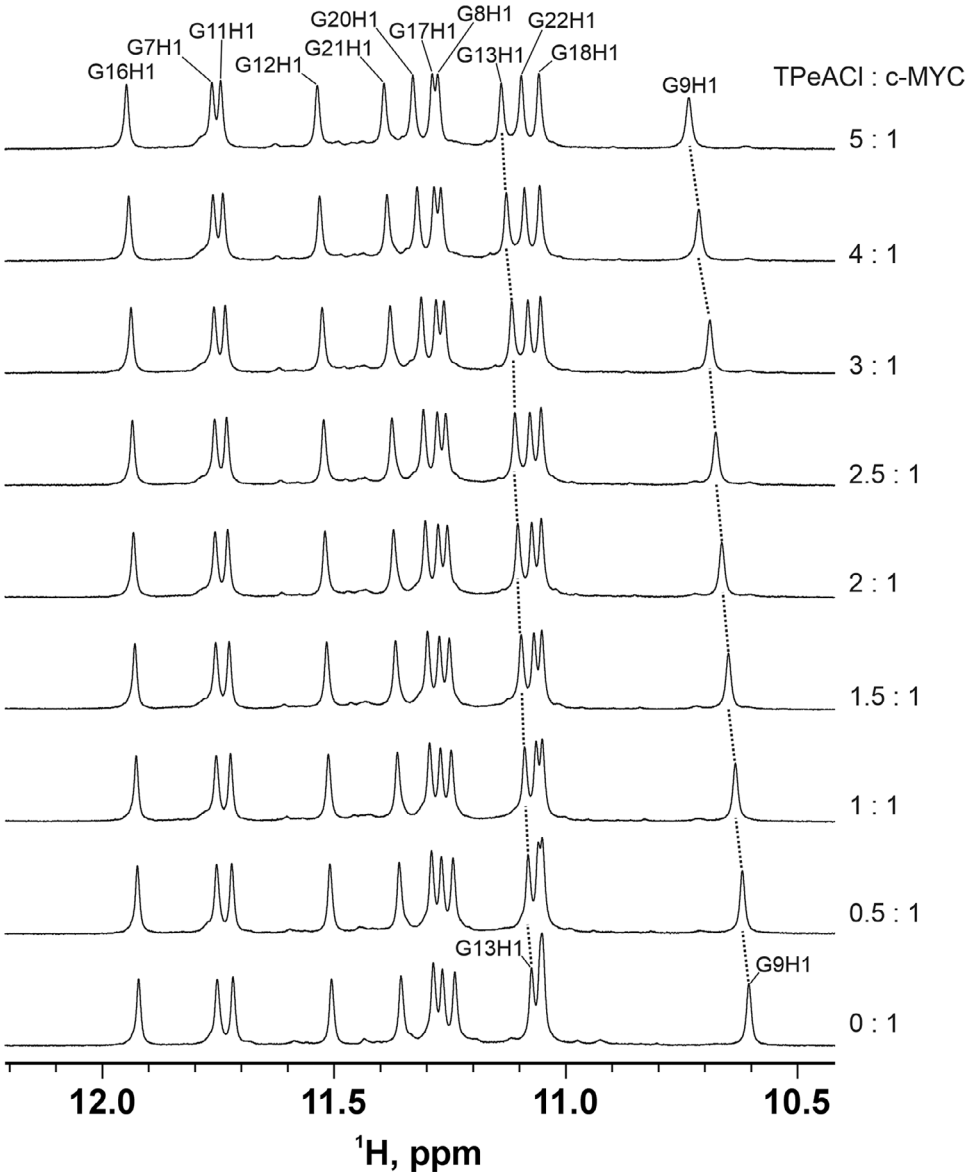

Figure 1. The imino spectral region of 1D ^{1}H NMR spectra of the c-MYC G-quadruplex at different concentrations of TPeACl. The spectrum was recorded in 90% H_2O, 10% D_2O, 20 mM KCl and 10 mM cesium phosphate buffer (pH 7.0) at 25 °C on a 600 MHz NMR spectrometer.

the human telomeric G-quadruplex or duplex DNA.[32] Analysis of the TAA^+-induced changes in melting temperature, T_M, has suggested that TAA^+ ions selectively bind to the c-MYC G-quadruplex with a one-to-one binding stoichiometry.[32] The stabilizing effect of TAA^+ ions on the c-MYC G-quadruplex, as characterized by the shift in the melting temperature, T_M, of the host structure, increases with the number of —CH_2— groups in the side chains with the greatest shift in T_M observed for solutions containing tetrapentylammonium ($TPeA^+$), *i.e.*, $[H(CH_2)_5]_4N^+$.[32] The markedly steep increase in the thermal stability of the c-MYC G-quadruplex with an increase in the concentration of $TPeA^+$ is consistent with complex formation and an estimated binding constant of $(2.2 \pm 0.5) \times 10^5$ M^{-1} at a T_M of 61.9 ± 0.5 °C.[32] This relatively tight binding coupled with a discriminatory power of TAA^+ ions with respect to G-quadruplex topology is remarkable considering their simple structure and the lack of aromatic groups, a property shared by all other classes of G-quadruplex-selective drugs.[21,24,31,33,34]

In this work, we continue this line of our studies by employing NMR spectroscopic, densimetric, and ultrasonic velocimetric measurements to characterize structurally and volumetrically the conjectured complex of $TPeA^+$ with the c-MYC G-quadruplex. NMR measurements reveal the structural features of the complex, while volumetric measurements shed light on changes in hydration and intrinsic dynamics of the G-quadruplex accompanying its complexation with $TPeA^+$.[35–42] Our NMR results suggest that $TPeA^+$ and c-MYC G-quadruplex indeed form a stable, one-to-one stoichiometric complex in which the ligand binds externally. These observations are in agreement with the predicted stoichiometry and the mode of binding, which were based on the analysis of the UV melting profiles and the examination of the CD spectra of the G-quadruplex in the absence

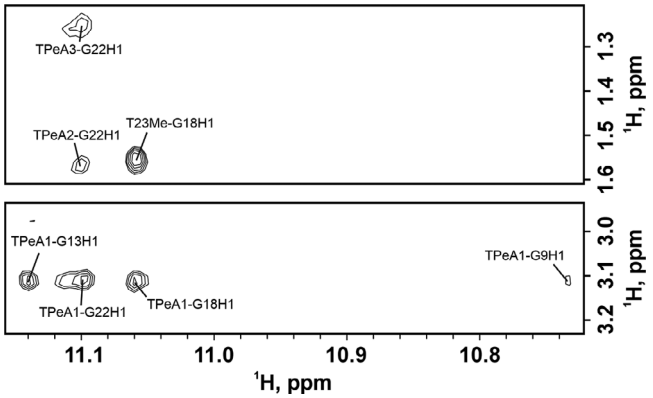

Figure 2. Two spectral regions of 2D NOESY NMR spectrum (mixing time = 200 ms) of 0.2 mM c-MYC G-quadruplex in the presence of 1.0 mM TPeACl (5:1 ligand-to-DNA ratio). The spectrum was recorded in 90% H_2O, 10% D_2O, 20 mM KCl and 10 mM cesium phosphate buffer (pH 7.0) at 25 °C on a 600 MHz NMR spectrometer.

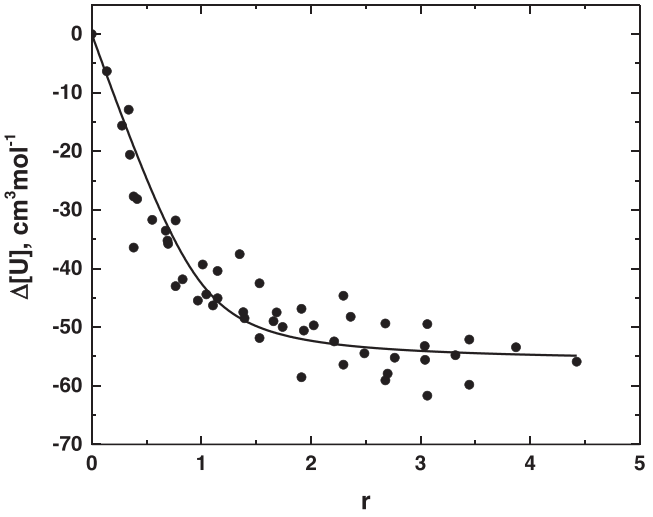

Figure 3. Changes in the relative molar sound velocity increment, Δ[U], of the c-MYC G-quadruplex plotted against the ligand-to-DNA, r. The concentration of the DNA was ~120 μM. The experimental points are fitted with Equation (1) (sold line).

and presence of $TPeA^+$.[32] In retrospect, this is an interesting development when a ligand-macromolecule complexation had been initially deduced from thermodynamic studies before its existence was subsequently verified structurally.

2. Results

2.1. NMR

1D ^{1}H NMR spectra of the $TPeA^+$-c-MYC G-quadruplex complex were recorded at different ligand-to-DNA ratios (Figure S1). The ^{1}H NMR spectra revealed 12 imino proton peaks corresponding to guanines involved in the three G-quartet planes of the c-MYC G-quadruplex, similar to those previously published for the MYC22-G14T/G23T G-quadruplex by Ambrus *et al.*[43] An increase in the concentration of $TPeA^+$ causes substantial changes in signal intensity and chemical shift in the following regions: (i) the imino spectral region of the 1D ^{1}H NMR spectrum, for the chemical shifts of G9H1 and G13H1 (Figure 1); (ii) the aromatic spectral region of the 1D ^{1}H NMR spectrum, for the chemical shifts of G22H8, T23H6, A24H2, A24H8, A25H2, and A25H8 (Figure S2); and (iii) the methyl spectral region of the 1D ^{1}H NMR spectrum, for the chemical shift of T23Me (Figure S3).

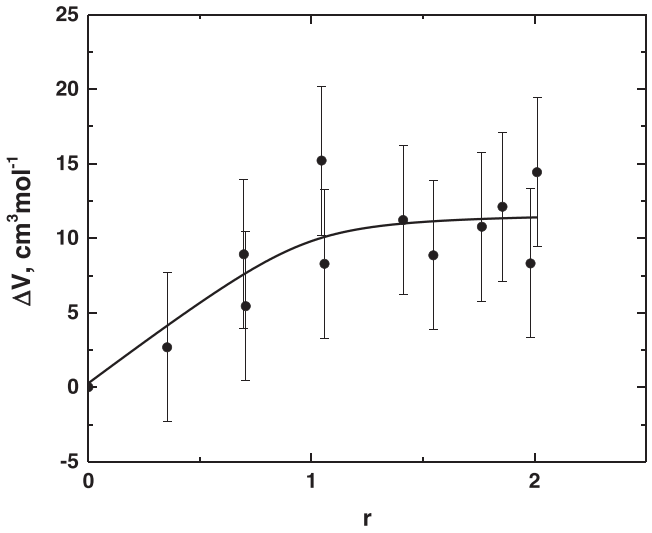

Figure 4. Changes in the partial molar volume, ΔV, of the c-MYC G-quadruplex plotted against the ligand-to-DNA ratio, r. The concentration of the DNA was ~120 μM. The experimental points are fitted with Equation (1) (sold line).

We performed 2D NMR measurements in 0.2 mM c-MYC G-quadruplex in the presence of 1.0 mM $TPeA^+$ ions (at a 5:1 ligand-to-DNA ratio) (Figures S4–S6). In the 2D NOESY NMR spectrum (with mixing time of 200 ms), there are several cross-peaks between $TPeA^+$ and imino protons of the G-quadruplex (Figure 2). Inspection of the 2D NOESY NMR spectrum of the $TPeA^+$-c-MYC G-quadruplex complex presented in Figure 2 (upper box) reveals that the CH_2 groups of the $TPeA^+$ ion at positions 2 and 3 both have cross-peaks with G22H1. Further inspection of Figure 2 (lower box) reveals that the CH_2 group of the $TPeA^+$ ion at position 1 has cross-peaks with G9H1, G13H1, G18H1, and G22H1. The ^{1}H DOSY spectrum presented in Figure S7 is consistent with the G-quadruplex being monomeric; in other words, no oligomerization occurs under our experimental conditions.

2.2. Ultrasonic Velocimetric and Densimetric Binding Profiles

Figure 3 shows the dependence of the relative molar sound velocity increment, $\Delta[U]$, of the c-MYC G-quadruplex on the $TPeA^+$-to-DNA ratio, r. Figure 4 shows a similar dependence for the partial molar volume, ΔV, of the G-quadruplex. Experimental points in Figures 3, 4 were fitted with a function describing a one-to-one stoichiometric binding of ligand to macromolecule[44]:

$$X = X_0 + \alpha \Delta X \quad (1)$$

Table 1. Solvent accessible surface areas, S_A, and intrinsic volumes, V_M, of the $TPeA^+$-c-MYC G-quadruplex complex, free G-quadruplex, and free ligand and the binding-induced changes in S_A and V_M.

	S_A, Å^2	V_M, Å^3	ΔS_A, Å^2	ΔV_M, Å^3
Complex	4723	6295	−686	198
c-MYC	4776	5776		
$TPeA^+$	633	321		

where X is an observable sensitive to the binding, such as relative molar sound velocity increment, $[U]$, and partial molal volume, V°; X_0 is the initial value of X at $r = 0$; ΔX is the asymptotic change in X at $r \rightarrow \infty$; $\alpha = 0.5(r+1) + \frac{1}{Y} + \sqrt{0.25(r-1)^2 + \frac{r+1}{Y} + \frac{1}{Y^2}}$ is the fractional population of ligated macromolecule; $Y = 2K_b[DNA]_T$; K_b is the binding constant; and $[DNA]_T$ is the total concentration of the DNA (macromolecule).

The fitted values of $\Delta[U]$ and K_b are -56 ± 2 cm^{3}mol^{-1} and $(0.85 \pm 0.35) \times 10^5$ M^{-1}, respectively. A binding constant, K_b, of $(0.85 \pm 0.35) \times 10^5$ M^{-1} determined at 25 °C is in reasonable agreement with $(2.2 \pm 0.5) \times 10^5$ M^{-1}, the value of K_b determined at 61.9 ± 0.5 °C from the ligand-induced shift in the melting temperature, T_M, of the host structure.[32]

The partial molar volume data shown in Figure 4 were fitted with Equation (1) with the binding constant, K_b, derived from the ultrasonic velocimetric data in Figure 3. The fitted value of ΔV is 11 ± 3 cm^{3}mol^{-1}. The values of $\Delta[U]$ and ΔV were combined in Equation (5) to calculate the binding-induced change in adiabatic compressibility: $\Delta K_S = 2\beta_{S0}(\Delta V - \Delta[U]) = (60 \pm 4) \times 10^{-4}$ cm^{3}mol^{-1}bar^{-1}.

2.3. Changes in Solvent-Accessible Surface Area and Intrinsic Volume

Table 1 lists the computed values of solvent-accessible surface area, S_A, and molecular volume, V_M, for the ligand-DNA complex (C), free ligand (L), and free DNA (DNA). The binding induced changes in solvent-accessible surface area, $\Delta S_A = S_A(C) - S_A(DNA) - S_A(L)$, and molecular volume, $\Delta V_M = V_M(C) - V_M(DNA) - V_M(L)$, are also shown in Table 1. The values of ΔS_A and ΔV_M equal −686 Å^2 and 198 Å^3, respectively.

3. Discussion

3.1. Structure

Figure 5 shows the structure of the $TPeA^+$-c-MYC G-quadruplex complex. The c-MYC DNA oligonucleotide forms a parallel-stranded G-quadruplex with three propeller loops and 5′-(T4-G5-A6) and 3′-(T23-A24-A25) flanking regions. There is a single binding site consistent with a one-to-one binding stoichiometry inferred from the analysis of the UV melting profiles of the G-quadruplex in the absence and presence of $TPeA^+$[32] and the ultrasonic velocimetric binding profile shown in Figure 3. In the

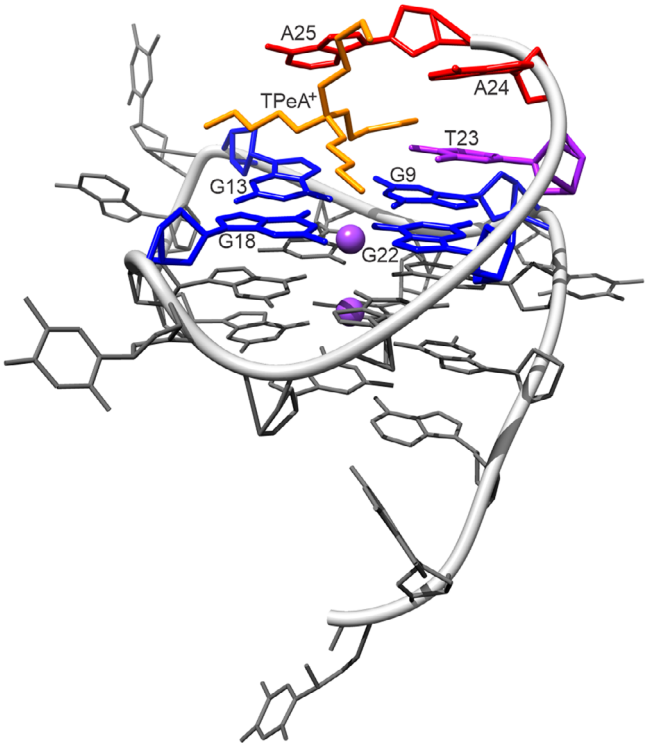

Figure 5. Structure of the complex between $TPeA^+$ and the c-MYC G-quadruplex. Guanine residues are shown in blue, adenine in red, thymidine in purple, $TPeA^+$ in orange, and the two potassium ions are displayed as purple spheres.

NOESY spectra (Figures 2, S4, S5), we observe weak cross-peaks between $TPeA^+$ and the 3′-end G-quartet residues, consistent with direct interaction at this site. We interpret the continued chemical shift perturbations observed at ligand excess as arising from broader changes in the chemical microenvironment of the G-quadruplex induced by bulk excess TPeACl, rather than additional specific binding sites. Minor changes in the chemical shifts ($\Delta\delta < 0.04$ ppm) of the imino protons of G8 and G17 (Figure 1) are not interpreted as reflecting a direct interaction with $TPeA^+$ but are attributed to secondary changes associated with the binding at the 3′-end G-quartet. $TPeA^+$ is positioned above the G9-G13-G18-G22 quartet of the c-MYC G-quadruplex and is surrounded by the 3′-(T23-A24-A25) flanking region. The binding does not cause appreciable changes in the structure of the G-quadruplex. This NMR result is consistent with the reported CD-spectral data suggesting that the binding is external with no changes in the structure of the host DNA.[32]

A closer look at the structure presented in Figure 5 suggests that the binding of $TPeA^+$ to the terminal G-quartet (G9-G13-G18-G22) would be sterically obstructed if a diagonal loop were present in the host G-quadruplex. This observation may explain why TAA^+ ions fail to bind to the basket-type antiparallel human telomeric G-quadruplex.[32] It is likely that steric repulsion between the diagonal loop of the basket-type antiparallel G-quadruplex and the side chains of the ligand prevents the binding.

3.2. Optimum Binding Geometry

We have previously shown that the affinity of the c-MYC G-quadruplex for TAA^+ ions, *i.e.*, $[H(CH_2)_n]_4N^+$, increases when the number of $—CH_2—$ groups within the side chains, *n*, increases from 1 to 5, while a further increase to 6 leads to a noticeable decrease in the affinity.[32] The structure of the $TPeA^+$-c-MYC complex shown in Figure 5 enables one to rationalize this observation. The affinity of TAA^+ ions for the c-MYC G-quadruplex appears to increase as the area of contact between the alkyl side chains of the ligand and the target G-quartet increases, which accompanies an increase in *n* from 1 to 5—gripping around the structure like the talons of a bird of prey. $TPeA^+$ covers the entire extent of the terminal G9-G13-G18-G22 G-quartet. A further increase in the number of $—CH_2—$ groups to 6 (in tetrahexylammonium) would extend the side chains beyond the limits of the G-quartet with no increase in contact area. Consequently, $TPeA^+$ exhibits the optimum binding to the c-MYC G-quadruplex.

3.3. Changes in Hydration

Hydration is a major force that dictates and modulates the structural features and binding properties of nucleic acids.[39,45–50] In recognition of this fact, considerable efforts have been invested to elucidate the role of water in the conformational stability of G-quadruplexes and their complexes.[51–58] Volumetric parameters are among the few which are sensitive to the entire population of waters of solute hydration; as such, they have been used to characterize hydration and changes in hydration accompanying folding transitions and binding events of nucleic acids.[37–39,42,46,59–70] A change in volume accompanying the association of a ligand with a macromolecule is the sum of the following contributions[71,72]:

$$\Delta V = \Delta V_M + \Delta V_T + \Delta V_I \quad (2)$$

where ΔV_M is the change in molecular volume; ΔV_T is the change in thermal volume; and ΔV_I is the change in interaction volume.

Thermal volume, V_T, is the volume of void space around the solute.[71,73] It is proportional to the solvent accessible surface area, S_A, of the solute with a coefficient of proportionality, δ, of ~0.5 Å.[71–73] Thus, $\Delta V_T = \delta \Delta S_A$. Interaction volume, V_I, is the change in the volume of solvent resulting from solute-solvent interactions.[71–73] It is related to solute hydration *via* $V_I = n_h(V_h - V_0)$ or $\Delta V_I = \Delta n_h(V_h - V_0)$, where n_h is the hydration number (the number of water molecules influenced by the solute), and V_0 and V_h are the partial molar volumes of bulk water and water of solute hydration, respectively.[35,72,73]

The computed value of ΔV_M in Equation (2) is 198 $Å^3$ (119 cm^3mol^{-1}) (Table 1). The magnitude of ΔV_T can be evaluated from $\Delta S_A = -686$ $Å^2$ (Table 1); $\Delta V_T = \delta \Delta S_A = 0.5 \times (-686) = -343$ $Å^3 = -207$ cm^3mol^{-1}. From Equation (2), a change in the interaction volume, ΔV_I, associated with the binding of $TPeA^+$ to the c-MYC G-quadruplex is $\Delta V_I = \Delta V - \Delta V_M - \Delta V_T = 11 - 119 + 207 = 99$ cm^3mol^{-1}. The positive sign of ΔV_I is consistent with an increase in the volume of solvent due to the binding-induced release of "electrostricted" waters of DNA hydration to the bulk. Electrostriction signifies a decrease in the partial molar volume of molecules of water solvating charged solutes under the influence of strong charge-dipole solute-solvent interactions.[74] The partial molar volume, V_h, of electrostricted molecules of water is ~10% smaller than that of bulk water; $(V_h - V_0) \approx -1.8$ cm^3mol^{-1}.[35,39,73]

Given $\Delta V_I = n_h(V_h - V_0)$, the number of water molecules released to the bulk can be calculated using $\Delta n_h = \frac{\Delta V_I}{V_h - V_0} = 99/(-1.8) = -55$. Thus, the binding of $TPeA^+$ to the c-MYC G-quadruplex causes a release of 55 waters of hydration to the bulk with a concomitant increase in the interaction volume, V_I.

3.4. Internal Dynamics

Dynamics is an important component of the stability and functioning of DNA, in general, and G-quadruplexes, in particular.[75–77] Compressibility can be used as a global measure of a change in dynamics accompanying the binding of $TPeA^+$ to the c-MYC G-quadruplex. The intrinsic coefficient of compressibility, β_M, of a macromolecule is related to its dynamics *via* the relationship[78,79]:

$$\langle V_M^2 \rangle = k_B T V_M \beta_M \quad (3)$$

where $\langle V_M^2 \rangle$ is the mean-square fluctuations of the intrinsic volume; k_B is Boltzmann's constant; and *T* is the temperature.

Information on the binding-induced change in the intrinsic coefficient of compressibility, β_M, of the c-MYC G-quadruplex can be gleaned from a change in compressibility, ΔK_S, accompanying its association with $TPeA^+$. The value of ΔK_S is the sum of changes in the hydration, $\Delta \Delta K_h$, and intrinsic, ΔK_M, contributions[35–38,73]:

$$\Delta K_S = \Delta K_M + \Delta \Delta K_h \quad (4)$$

In Equation (4), $K_M = \beta_M V_M$ is the intrinsic compressibility of the macromolecule. The hydration contribution, $\Delta K_h = n_h(K_h - K_0)$, is the change in the compressibility of water due to solute-solvent interactions, and K_0 and K_h are the partial molar adiabatic compressibilities of bulk water and water of solute hydration, respectively.

The partial molar adiabatic compressibility, K_h, of water hydrating a charged solute is ~25% smaller than that of bulk water, K_0; hence $(K_h - K_0) \approx -2 \times 10^{-4}$ $cm^3mol^{-1}bar^{-1}$.[35,39,73] With this value and the volume-based estimate of Δn_h, we evaluate $\Delta \Delta K_h = \Delta n_h(K_h - K_0) = (-55) \times (-2 \times 10^{-4}) = 110 \times 10^{-4}$ $cm^3mol^{-1}bar^{-1}$. The positive sign of $\Delta \Delta K_h$ is consistent with an increase in the compressibility of solvent resulting from the release to the bulk of low-compressible waters of DNA hydration.[35–37,39]

The binding-induced change in the intrinsic compressibility, K_M, of the G-quadruplex can be estimated from Equation (4) as $\Delta K_M = \Delta K_S - \Delta \Delta K_h = 60 \times 10^{-4} - 110 \times 10^{-4} = -50 \times 10^{-4}$ $cm^3mol^{-1}bar^{-1}$. Thus, the association with $TPeA^+$

leads to a decrease in the intrinsic compressibility of the c-MYC G-quadruplex. This result is in concert with the sign of changes in intrinsic compressibility observed in previous studies of ligand binding to proteins and DNA.[44,62,80–82] Rigidification of the host macromolecule appears to be a common feature of ligand-macromolecule binding events.

A change in intrinsic compressibility, K_M ($= \beta_M V_M$), is given by $\Delta K_M = \Delta\beta_M V_M + \beta_M \Delta V_M$. Since the binding of $TPeA^+$ to the c-MYC G-quadruplex is external with little, if any, alteration in structure, a change in the intrinsic volume of the DNA, ΔV_M, should be small (close to 0). Thus, $\Delta K_M \approx \Delta\beta_M V_M$ and $\Delta\beta_M = \Delta K_M / V_M$. With the molecular volume, V_M, of the c-MYC G-quadruplex being 5776 Å^3 or 3478 cm^{3}mol^{-1} (Table 1), we calculate $\Delta\beta_M = \Delta K_M / V_M = -50 \times 10^{-4} / 3478 = -1.4 \times 10^{-6}$ bar^{-1}.

Inspection of Equation (3) reveals that a decrease in β_M is consistent with the binding-induced reduction in the mean-square fluctuations of the intrinsic volume, $\langle V_M^2 \rangle$, of the G-quadruplex. The intrinsic coefficient of compressibility, β_M, of a G-quadruplex has not been determined as of yet. Therefore, it is not possible to estimate the relative magnitude of the binding-induced change in $\langle V_M^2 \rangle$. However, G-quadruplexes are globular structures with an intramolecular void, in that sense resembling small globular proteins. The intrinsic coefficient of compressibility, β_M, of a globular protein is on the order of $\sim 25 \times 10^{-6}$ bar^{-1}.[83–85] If one suggests that, by analogy, the value of β_M of a G-quadruplex is not much different from that of a globular protein, our determined value of $\Delta\beta_M$ (-1.4×10^{-6} bar^{-1}) should be on the order of 5% of β_M. Hence, as a plausible estimate, the binding of $TPeA^+$ to the c-MYC G-quadruplex causes a ~5% decrease in dynamics as characterized by volume fluctuations.

The intrinsic compressibility, β_M, of a G-quadruplex is likely to differ from that of a globular protein (25×10^{-6} bar^{-1}). However, even if the difference is twofold in either direction, the ratio $\Delta\beta_M/\beta_M$ and, hence, the relative change in dynamic, $\Delta\langle V_M^2 \rangle / \langle V_M^2 \rangle$, still should be within 2–10%. Thus, the association of $TPeA^+$ with the c-MYC G-quadruplex is accompanied by only a moderate diminution in dynamics. This observation is consistent with the external mode of binding of $TPeA^+$ to the c-MYC G-quadruplex that does not cause significant changes in the structure of the host.

4. Conclusion

We previously have shown that TAA^+ ions, *i.e.*, $[H(CH_2)_n]_4N^+$, strongly stabilize the parallel c-MYC G-quadruplex while not influencing the thermal stabilities of the antiparallel human telomeric G-quadruplex or duplex DNA.[32] Based on these observations, we proposed that TAA^+ ions bind to the c-MYC G-quadruplex with the strongest binding exhibited by $TPeA^+$, *i.e.*, $[H(CH_2)_5]_4N^+$.[32] In the present work, we continue our exploration of this novel paradigm of selective G-quadruplex recognition by performing NMR spectroscopic and volumetric characterization of the $TPeA^+$-c-MYC G-quadruplex complex.

Our NMR results revealed that, $TPeA^+$ indeed forms a stable complex with the c-MYC G-quadruplex in which $TPeA^+$ is positioned above the terminal G9-G13-G18-G22 quartet and is surrounded by the 3′-(T23-A24-A25) flanking region. The external mode of binding and the absence of binding-induced alterations in the structure of the host DNA are in agreement with the reported CD spectral data.[32] Our densimetric and ultrasonic velocimetric measurements revealed that the binding of $TPeA^+$ to the c-MYC G-quadruplex is accompanied by increases in volume, ΔV, and adiabatic compressibility, ΔK_S, of 11 ± 3 cm^{3}mol^{-1} and $(60 \pm 4) \times 10^{-4}$ cm^{3}mol^{-1}bar^{-1}, respectively. The value of ΔV was combined with changes in solvent-accessible surface area and molecular volume computed from structural data to evaluate the number of water molecules released to the bulk, Δn_h. The binding of $TPeA^+$ to the c-MYC G-quadruplex is accompanied by a release of 55 water molecules. By combining the values of ΔK_S and Δn_h, we estimated a ~5% decrease in G-quadruplex dynamics as expressed by the mean-square fluctuations of intrinsic volume, $\langle V_M^2 \rangle$. The observed moderate change in dynamics is consistent with the external mode of binding and the absence of structural alterations in the host G-quadruplex. Taken together, the structural and physico-chemical insights emerging from this investigation and our previous work[32] lay the foundation for further studies of TAA^+-based compounds as a possible point of departure for designing topology-sensitive G-quadruplex-binding agents.

5. Experimental

Materials: The c MYC22-G14T/G23T DNA oligonucleotide d(TGA GGGTGGGTAGGGTGGGTAA), that was used for NMR and volumetric measurements, had come from two different sources. The sample used for NMR studies was synthesized on a K&A Laborgeräte model H8 DNA/RNA Synthesizer (Schaafheim, Germany) using standard phosphoramidite solid phase chemistry with DMT-on protection according to the manufacturer's protocol. The oligonucleotide was prepared at natural isotope abundance using products from Cambridge Isotope Laboratories (Tewksbury, MA, USA). Following the synthesis, the oligonucleotide was deprotected overnight in concentrated aqueous ammonia at 55 °C and purified using Glen-Pak DNA cartridges (Sterling, VA, USA). Samples were dried in vacuo and redissolved for desalting in 200 mM LiCl in deionized Milli-Q water using Amicon Ultra-15 centrifugal filters with a cut-off of 3 kDa.

NMR measurements were performed at pH 7.0 in a 10 mM cesium phosphate buffer with 20 mM potassium chloride (KCl) prepared with 90% H_2O and 10% D_2O. NMR samples with different ligand-to-DNA ratios were prepared by adding aliquots of a stock solution of 35 mM TPeACl to the DNA.

For volumetric measurements, the oligonucleotide was purchased from Integrated DNA Technologies (Coralville, IA, USA). The DNA was dissolved in 10 mM cesium chloride, dialyzed exhaustively against distilled water in Tube-O-Dialyzers (2000-Da cut-off, G Biosciences, St. Louis, MO), and lyophilized. The lyophilized DNA was subsequently dissolved in a 10 mM cesium phosphate buffer adjusted to pH 7.0 and supplemented with 20 mM KCl. The concentrations of the DNA for the NMR and volumetric measurements were on the order of ~200 and ~120 μM, respectively.

KCl, cesium hydroxide monohydrate, phosphoric acid, and $TPeA^+$ chloride (TPeACl) were purchased from Sigma-Aldrich Canada (Oakville, ON, Canada), Sigma-Aldrich (St. Louis, MO, USA), or MedChemExpress (Monmouth Junction, NJ, USA). All reagents were of the highest commercially available grade and used

without further purification. The solutions were prepared with doubly distilled water.

The concentrations of DNA samples were determined spectrophotometrically with either a Jasco model V-730 UV-Vis spectrophotometer (Easton, MD, USA) or a Cary 3500 UV-Vis spectrophotometer (Agilent, Santa Clara, CA, USA) and a molar extinction coefficient, ε_{260}, of 228700 $M^{-1}cm^{-1}$ for the unfolded state. The latter was computed using a nearest-neighbor procedure described by Owczarzy.[86]

NMR Spectroscopy: NMR data were collected on a 600 MHz Bruker AVANCE NEO NMR spectrometer (Bruker BioSpin, Ettlingen, Germany) using a 5 mm TCI (proton-optimized triple resonance NMR) cryoprobe at 25 °C. Excitation-sculpting pulse sequence with gradients was used for water suppression. A relaxation delay of 1.0 s was used for 1D ^{1}H NMR spectra and 3.0 s for 2D NMR spectra. 2D NOESY spectra were acquired with a mixing time of 200 ms, while 2D ROESY spectrum was acquired with a mixing time of 80 ms. All NMR spectra were referenced to DSS. The spectra were processed and analyzed using Topspin 4 (Bruker BioSpin, Ettlingen, Germany) and Sparky (UCSF, San Francisco, CA, USA) software.

Structure calculations: AmberTools25 (UCSF, San Francisco, CA, USA) was used to model the $TPeA^+$-c-MYC G-quadruplex complex. The 3D structure of c-MYC (PDB ID 1XAV) served as the starting c-MYC DNA conformation and was parameterized with the bsc1 (OL15) force field for nucleic acids. The ligand was parameterized with Antechamber using the GAFF2 force field, and partial atomic charges were assigned by the AM1-BCC method. No additional frcmod corrections were required; the ligand MOL2 parameter file is provided in Supporting Information. The complex was assembled in tleap and solvated in a cubic TIP3P water box with a 12 Å buffer in all directions. Potassium counterions were added to neutralize the system.

NMR-derived distance restraints were applied to preserve the hydrogen-bonding pattern observed in the 2D NOESY spectrum. The *anti* configuration of the G-quartets was determined experimentally from the intensity of the H1′-H8 cross-peaks, and a modest planarity restraint (20 kcal $mol^{-1}Å^{-2}$) was applied to the G-quartets. The distances between $TPeA^+$ and the imino protons of the c-MYC DNA were restricted to $\leq$ 5 Å. The complete restraint input file is provided in Supporting Information.

Energy minimization with restraints was performed in two stages: 1500 steps of steepest descent followed by 1500 steps of conjugate gradient. Molecular dynamics simulations with restraints were then run for 50000 steps (100 ps) under NVT ensemble conditions at 300 K, controlled by a Langevin thermostat. Electrostatic interactions were treated with the Particle Mesh Ewald (PME) method under periodic boundary conditions, with a 10 Å cutoff for nonbonded short-range interactions. The SHAKE algorithm was applied to constrain bonds involving hydrogen atoms, with a 2 fs integration time step. The final structures were obtained by an additional 1000 steps of unrestrained minimization, and a representative conformation was extracted using cpptraj.

High precision densimetry and ultrasonic velocimetry: The densities of solutions of the c-MYC G-quadruplex in the absence and presence of TPeACl were measured at 25 °C with a precision of $\pm$ 1.5 $\times$ 10^{-6} g cm^{-3}. All density measurements were conducted using an Anton Paar model DMA-5000 vibrating tube densimeter (Graz, Austria). The partial molar volume, V°, of the G-quadruplex was computed from $V^\circ = \frac{M}{\rho_0} - \frac{\rho - \rho_0}{\rho_0 C}$, where ρ and ρ_0 are the densities of the DNA solution and the neat solvent, respectively; C is the molar concentration of the DNA; and M is the molecular weight of the DNA.

Solution sound velocities were measured at 25 °C with the resonator method and a differential technique at a frequency of 7.2 MHz.[87–89] The frequency characteristics of the resonator cells required to determine sound velocity were analyzed with a Hewlett Packard model E5100A network/spectrum analyzer (Mississauga, ON, Canada). The relative precision of sound velocity measurements provided by the ultrasonic resonator used in this work is on the order $\pm$ 1 $\times$ 10^{-4}%.[89] The measured acoustic property of a solute is its relative molar sound velocity increment, $[U] = \frac{U - U_0}{U_0 C}$, where U and U_0 are the sound velocities in the DNA solution and the neat solvent, respectively.

The partial molar adiabatic compressibility, K°_S, of a solute can be computed by combining the relative molar sound velocity increment, $[U]$, and partial molar volume, V°, from the relationship[90–92]:

$$K^\circ_S = \beta_{S0}\left(2V^\circ - 2[U] - \frac{M}{\rho_0}\right) \quad (5)$$

where β_{S0} is the coefficient of adiabatic compressibility of the solvent.

In volumetric titration experiments, aliquots of the $TPeA^+$ chloride (~10 mM) were added to the initial solution containing the c-MYC G-quadruplex (~0.12 mM). Densimetric and acoustic titrations were performed as previously described in triplicate.[93]

Computation of the Binding-induced Changes in Solvent-accessible Surface Area, ΔS_A, and Intrinsic Volume, ΔV_M: We computed the values of ΔV_M and ΔS_A as the difference in V_M or S_A between the $TPeA^+$-c-MYC G-quadruplex complex and the sum of V_M or S_A of the free ligand and the free DNA. The atomic coordinates of the complex were taken from our NMR structure. We used it to calculate the intrinsic volumes, V_M, and solvent accessible surface areas, S_A, for the ligand-G-quadruplex complex, free G-quadruplex, and free ligand.

To calculate solvent-accessible surface areas and molecular volumes, we employed two programs: MoloVol version 1.2.1 (obtained from https://molovol.com)[94] and ProteinVolume version 1.3 (obtained from https://gmlab.bio.rpi.edu/).[95] To validate and verify our results, we additionally calculated solvent-accessible surface areas using FreeSASA version 2.1.2 (obtained from https://freesasa.github.io/)[96] and VMD version 1.9.4a53 (obtained from https://www.ks.uiuc.edu/Research/vmd/).[97] In all calculations, hydrogens atoms were ignored. A spherical probe with a radius of 1.4 Å was used for all programs except for ProteinVolume. The latter recommends, as the default, a volume probe radius of 0.080–0.020 Å and a surface probe minimum distance of 0.1 Å.

Supporting Information

1D ^{1}H NMR spectra of c-MYC DNA oligonucleotide at different concentrations of TPeACl. (a) δ_H 12.5–4.8 ppm region, (b) δ_H 4.8–0.5 ppm region. The spectrum was recorded in 90% H_2O, 10% D_2O, 20 mM KCl and 10 mM cesium phosphate buffer (pH 7.0) at 25 °C on a 600 MHz NMR spectrometer (Figure S1); the aromatic spectral region of 1D ^{1}H NMR spectra of c-MYC DNA oligonucleotide at different TPeACl concentrations. The spectrum was recorded in 90% H_2O, 10% D_2O, 20 mM KCl, and 10 mM cesium phosphate buffer (pH 7.0) at 25 °C on a 600 MHz NMR spectrometer (Figure S2); the methyl spectral region of 1D ^{1}H NMR

spectra of c-MYC DNA oligonucleotide at different TPeACl concentrations. The spectrum was recorded in 90% H_2O, 10% D_2O, 20 mM KCl, and 10 mM cesium phosphate buffer (pH 7.0) at 25 °C on a 600 MHz NMR spectrometer (Figure S3); 2D NOESY NMR spectrum (mixing time = 200 ms) of 0.2 mM c-MYC DNA oligonucleotide in the presence of 1.0 mM TPeACl (5:1 ligand-to-DNA ratio). The spectrum was recorded in 90% H_2O, 10% D_2O, 20 mM KCl, and 10 mM cesium phosphate buffer (pH 7.0) at 25 °C on a 600 MHz NMR spectrometer (Figure S4); 2D NOESY NMR spectrum (mixing time = 200 ms) of 0.05 mM c-MYC DNA oligonucleotide in the presence of 0.25 mM TPeACl (5:1 ligand-to-DNA ratio). The spectrum was recorded in 90% H_2O, 10% D_2O, 20 mM KCl, and 10 mM cesium phosphate buffer (pH 7.0) at 25 °C on a 600 MHz NMR spectrometer (Figure S5); 2D ROESY NMR spectrum (ROESY spin-lock = 80 ms) of 0.2 mM c-MYC DNA oligonucleotide in the presence of 1.0 mM TPeACl (5:1 ligand-to-DNA ratio). The spectrum was recorded in 90% H_2O, 10% D_2O, 20 mM KCl, and 10 mM cesium phosphate buffer (pH 7.0) at 25 °C on a 600 MHz NMR spectrometer (Figure S6); ^{1}H DOSY NMR spectrum of 0.2 mM c-MYC DNA oligonucleotide in the presence of 1.0 mM TPeACl (5:1 ligand-to-DNA ratio). The spectrum was recorded in 90% H_2O, 10% D_2O, 20 mM KCl, and 10 mM cesium phosphate buffer (pH 7.0) at 25 °C on a 600 MHz NMR spectrometer (Figure S7). The restraint input file, "restraints.txt", is used in AMBER calculations. The ligand MOL2 parameter file, "ligand.mol2", is the input file of $TPeA^+$ ion.

Acknowledgments

The authors gratefully acknowledge many stimulating discussions with Prof. Robert B. Macgregor, Jr., and the financial support from the Leslie Dan Faculty of Pharmacy of the University of Toronto and the Slovenian Research and Innovation Agency (ARIS, Grants P1-0242 and J1-60019). The authors acknowledge the CERIC-ERIC consortium for the access to experimental facilities and financial support.

Author Contributions

J.P. and T.V.C. designed research; X.L. and M.C. performed research; X.L., M.C., D.N.D., J.P., and T.V.C. analyzed data; and J.P. and T.V.C. wrote the paper.

Notes

The authors declare no competing financial interest.

Conflict of Interest

The authors declare no conflict of interest.

Data Availability Statement

The data that support the findings of this study are available from the corresponding authors upon reasonable request.

Keywords: compressibility · G-quadruplexes · NMR · tetrapentylammonium · volume

[1] S. Balasubramanian, L. H. Hurley, S. Neidle, *Nat. Rev. Drug Disc.* **2011**, *10*, 261.
[2] A. N. Lane, J. B. Chaires, R. D. Gray, J. O. Trent, *Nucleic Acids Res.* **2008**, *36*, 5482.
[3] H. Tateishi-Karimata, N. Sugimoto, *Chem. Commun.* **2020**, *56*, 2379.
[4] S. Takahashi, N. Sugimoto, *Acc. Chem. Res.* **2021**, *54*, 2110.
[5] R. C. Monsen, J. O. Trent, J. B. Chaires, *Acc. Chem. Res.* **2022**, *55*, 3242.
[6] J. Plavec, in *Handbook of Chemical Biology of Nucleic Acids* (Ed.: N. Sugimoto), Springer Nature, Singapore, **2023**, pp. 169–212.
[7] N. Medved, M. Cevec, U. Javornik, J. Lah, S. Hadzi, J. Plavec, *Angew. Chem. Int. Ed.* **2025**, *64*, e202507544.
[8] S. Aleksic, P. Podbevsek, J. Plavec, *Nucleic Acids Res.* **2025**, *53*, gkaf260.
[9] M. Trajkovski, A. Pastore, J. Plavec, *Nucleic Acids Res.* **2024**, *52* 1591.
[10] T. Fujii, P. Podbevsek, J. Plavec, N. Sugimoto, *J. Inorg. Biochem.* **2017**, *166* 190.
[11] A. Ghosh, M. Trajkovski, M. P. Teulade-Fichou, V. Gabelica, J. Plavec, *Angew. Chem. Int. Ed.* **2022**, *61*, e202207384.
[12] M. L. Bochman, K. Paeschke, V. A. Zakian, *Nat. Rev. Genet.* **2012**, *13*, 770.
[13] D. Varshney, J. Spiegel, K. Zyner, D. Tannahill, S. Balasubramanian, *Nat. Rev. Mol. Cell Biol.* **2020**, *21*, 459.
[14] J. Spiegel, S. Adhikari, S. Balasubramanian, *Trends Chem* **2020**, *2*, 123.
[15] H. Tateishi-Karimata, N. Sugimoto, *Nucleic Acids Res.* **2021**, *49*, 7839.
[16] P. Obara, P. Wolski, T. Panczyk, *Molecules* **2024**, *29*, 4683.
[17] L. Liu, C. Ma, J. W. Wells, T. V. Chalikian, *J. Phys. Chem. B* **2020**, *124*, 751.
[18] L. Liu, L. Zhu, H. Tong, C. Su, J. W. Wells, T. V. Chalikian, *J. Phys. Chem. B* **2022**, *126*, 6654.
[19] A. Garabet, I. Prislan, N. Poklar Ulrih, J. W. Wells, T. V. Chalikian, *Biomolecules* **2025**, *15*, 483.
[20] J. W. Wells, T. V. Chalikian, *Q. Rev. Biophys. Discovery* **2025**, *6*, e24.
[21] S. Neidle, *J. Med. Chem.* **2016**, *59*, 5987.
[22] S. Neidle, *Molecules* **2024**, *29*, 3653.
[23] L. Chen, J. Dickerhoff, S. Sakai, D. Yang, *Acc. Chem. Res.* **2022**, *55*, 2628.
[24] J. Figueiredo, J. L. Mergny, C. Cruz, *Life Sci.* **2024**, *340*, 122481.
[25] J. Husby, A. K. Todd, J. A. Platts, S. Neidle, *Biopolymers* **2013**, *99*, 989.
[26] S. A. Ohnmacht, C. Marchetti, M. Gunaratnam, R. J. Besser, S. M. Haider, G. Di Vita, H. L. Lowe, M. Mellinas-Gomez, S. Diocou, M. Robson, J. Sponer, B. Islam, R. B. Pedley, J. A. Hartley, S. Neidle, *Sci. Rep.* **2015**, *5*, 11385.
[27] L. Savva, S. N. Georgiades, *Molecules* **2021**, *26*, 841.
[28] N. W. Luedtke, *Chimia* **2009**, *63*, 134.
[29] G. W. Collie, G. N. Parkinson, *Chem. Soc. Rev.* **2011**, *40*, 5867.
[30] Y. Ma, K. Iida, K. Nagasawa, *Biochem. Biophys. Res. Commun.* **2020**, *531*, 3.
[31] T. Biver, *Molecules* **2022**, *27*, 4165.
[32] X. Li, D. N. Dubins, J. Volker, T. V. Chalikian, *J. Phys. Chem. B* **2024**, *128*, 11144.
[33] I. Alessandrini, M. Recagni, N. Zaffaroni, M. Folini, *Int. J. Mol. Sci.* **2021**, *22*, 5947.
[34] N. Kosiol, S. Juranek, P. Brossart, A. Heine, K. Paeschke, *Mol. Cancer* **2021**, *20*, 40.
[35] T. V. Chalikian, *J. Phys. Chem. B* **2001**, *105*, 12566.
[36] T. V. Chalikian, A. P. Sarvazyan, K. J. Breslauer, *Biophys. Chem.* **1994**, *51*, 89.
[37] T. V. Chalikian, K. J. Breslauer, *Biopolymers* **1998**, *48*, 264.
[38] T. V. Chalikian, K. J. Breslauer, *Curr. Opin. Struct. Biol.* **1998**, *8*, 657.
[39] T. V. Chalikian, R. B. Macgregor, *Phys. Life Rev.* **2007**, *4*, 91.
[40] T. V. Chalikian, R. B. Macgregor, Jr., *Biology* **2021**, *10*, 813.
[41] T. V. Chalikian, *J. Mol. Liq.* **2023**, *385*, 122320.
[42] T. V. Chalikian, R. B. Macgregor, Jr., in *Handbook of Chemical Biology of Nucleic Acids* (Ed.: N. Sugimoto), Springer Nature, Singapore, **2023**, pp. 81–111.

[43] A. Ambrus, D. Chen, J. X. Dai, R. A. Jones, D. Z. Yang, *Biochemistry* **2005**, *44*, 2048.
[44] I. Son, Y. L. Shek, D. N. Dubins, T. V. Chalikian, *Biochemistry* **2012**, *51*, 5784.
[45] T. V. Chalikian, J. Volker, in *Wiley Encyclopedia of Chemical Biology* (Ed.: T. P. Begley), Wiley and Sons, Inc., Hoboken, NJ, **2008**.
[46] I. Son, Y. L. Shek, D. N. Dubins, T. V. Chalikian, *J. Am. Chem. Soc.* **2014**, *136*, 4040.
[47] S. Nakano, D. Yamaguchi, H. Tateishi-Karimata, D. Miyoshi, N. Sugimoto, *Biophys. J.* **2012**, *102*, 2808.
[48] S. Ghosh, S. Takahashi, T. Ohyama, L. Liu, N. Sugimoto, *J. Am. Chem. Soc.* **2024**, *146*, 32479.
[49] S. Nakano, D. Miyoshi, N. Sugimoto, *Chem. Rev.* **2014**, *114*, 2733.
[50] W. Saenger, W. N. Hunter, O. Kennard, *Nature* **1986**, *324*, 385.
[51] K. Li, L. Yatsunyk, S. Neidle, *Nucleic Acids Res.* **2021**, *49*, 519.
[52] S. Matsumoto, S. Takahashi, S. Bhowmik, T. Ohyama, N. Sugimoto, *Anal. Chem.* **2022**, *94*, 7400.
[53] D. Miyoshi, H. Karimata, N. Sugimoto, *J. Am. Chem. Soc.* **2006**, *128*, 7957.
[54] S. Nagatoishi, N. Isono, K. Tsumoto, N. Sugimoto, *ChemBioChem* **2011**, *12*, 1822.
[55] H. Y. Fan, Y. L. Shek, A. Amiri, D. N. Dubins, H. Heerklotz, R. B. Macgregor, T. V. Chalikian, *J. Am. Chem. Soc.* **2011**, *133*, 4518.
[56] S. Takahashi, S. Bhowmik, N. Sugimoto, *J. Inorg. Biochem.* **2017**, *166*, 199.
[57] Y. Y. Li, D. N. Dubins, D. Le, K. Leung, R. B. Macgregor, Jr., *Biophys. Chem.* **2017**, *231*, 55.
[58] S. Takahashi, N. Sugimoto, *Biophys. Chem.* **2017**, *231*, 146.
[59] T. V. Chalikian, G. E. Plum, A. P. Sarvazyan, K. J. Breslauer, *Biochemistry* **1994**, *33*, 8629.
[60] F. Han, T. V. Chalikian, *J. Am. Chem. Soc.* **2003**, *125*, 7219.
[61] F. Han, N. Taulier, T. V. Chalikian, *Biochemistry* **2005**, *44*, 9785.
[62] L. Liu, L. Stepanian, D. N. Dubins, T. V. Chalikian, *J. Phys. Chem. B* **2018**, *122*, 7647.
[63] Y. L. Shek, G. D. Noudeh, M. Nazari, H. Heerklotz, R. M. Abu-Ghazalah, D. N. Dubins, T. V. Chalikian, *Biopolymers* **2014**, *101*, 216.
[64] G. I. Makhatadze, C. R. Chen, I. Khutsishvili, L. A. Marky, *Biophys. J.* **2022**, *121*, 4892.
[65] T. V. Chalikian, J. Volker, A. R. Srinivasan, W. K. Olson, K. J. Breslauer, *Biopolymers* **1999**, *50*, 459.
[66] T. V. Chalikian, J. Volker, G. E. Plum, K. J. Breslauer, *Proc. Natl. Acad. Sci. U. S. A.* **1999**, *96*, 7853.
[67] D. N. Dubins, A. Lee, R. B. Macgregor, Jr., T. V. Chalikian, *J. Am. Chem. Soc.* **2001**, *123*, 9254.
[68] G. R. Hedwig, H. Hoiland, *J. Solution Chem.* **2017**, *46*, 849.
[69] V. A. Buckin, B. I. Kankiya, N. V. Bulichov, A. V. Lebedev, I. Y. Gukovsky, V. P. Chuprina, A. P. Sarvazyan, A. R. Williams, *Nature* **1989**, *340*, 321.
[70] B. I. Kankia, L. A. Marky, *J. Am. Chem. Soc.* **2001**, *123*, 10799.
[71] D. P. Kharakoz, *J. Solution Chem.* **1992**, *21*, 569.
[72] T. V. Chalikian, R. Filfil, *Biophys. Chem.* **2003**, *104*, 489.
[73] T. V. Chalikian, R. B. Macgregor, Jr., *Biophys. Chem.* **2019**, *246*, 8.
[74] Y. Marcus, *Chem. Rev.* **2011**, *111*, 2761.
[75] B. Ashwood, A. Tokmakoff, *Nat. Rev. Chem.* **2025**, *9*, 305.
[76] Y. Cheng, Y. Zhang, H. You, *Biomolecules* **2021**, *11*, 1579.
[77] P. A. Summers, B. W. Lewis, J. Gonzalez-Garcia, R. M. Porreca, A. H. M. Lim, P. Cadinu, N. Martin-Pintado, D. J. Mann, J. B. Edel, J. B. Vannier, M. K. Kuimova, R. Vilar, *Nat. Commun.* **2021**, *12*, 162.
[78] A. Cooper, *Proc. Natl. Acad. Sci. U. S. A.* **1976**, *73*, 2740.
[79] A. Cooper, *Prog. Biophys. Mol. Biol.* **1984**, *44*, 181.
[80] D. N. Dubins, R. Filfil, R. B. Macgregor, T. V. Chalikian, *J. Phys. Chem. B* **2000**, *104*, 390.
[81] R. Filfil, T. V. Chalikian, *FEBS Lett.* **2003**, *554*, 351.
[82] I. Son, R. Selvaratnam, D. N. Dubins, G. Melacini, T. V. Chalikian, *J. Phys. Chem. B* **2013**, *117*, 10779.
[83] T. V. Chalikian, M. Totrov, R. Abagyan, K. J. Breslauer, *J. Mol. Biol.* **1996**, *260*, 588.
[84] T. V. Chalikian, *Annu. Rev. Biophys. Biomol. Struct.* **2003**, *32*, 207.
[85] N. Taulier, T. V. Chalikian, *Biochim. Biophys. Acta* **2002**, *1595*, 48.
[86] A. V. Tataurov, Y. You, R. Owczarzy, *Biophys. Chem.* **2008**, *133*, 66.
[87] F. Eggers, T. Funck, *Rev. Sci. Instrum.* **1973**, *44*, 969.
[88] F. Eggers, *Acustica* **1992**, *76*, 231.
[89] A. P. Sarvazyan, *Ultrasonics* **1982**, *20*, 151.
[90] S. Barnartt, *J. Chem. Phys.* **1952**, *20*, 278.
[91] B. B. Owen, H. L. Simons, *J. Phys. Chem.* **1957**, *61*, 479.
[92] A. P. Sarvazyan, *Annu. Rev. Biophys. Biophys. Chem.* **1991**, *20*, 321.
[93] T. V. Chalikian, V. S. Gindikin, K. J. Breslauer, *J. Mol. Biol.* **1995**, *250*, 291.
[94] J. B. Maglic, R. Lavendomme, *J. Appl. Crystallogr.* **2022**, *55*, 1033.
[95] C. R. Chen, G. I. Makhatadze, *BMC Bioinfo* **2015**, *16*, 101.
[96] S. Mitternacht, *F1000Res* **2016**, *5*, 189.
[97] W. Humphrey, A. Dalke, K. Schulten, *J. Mol. Graph.* **1996**, *14*, 33.

Manuscript received: August 27, 2025
Revised manuscript received: October 9, 2025
Version of record online: October 27, 2025